Chemical Engineering Journal 154 (2009) 94–106

Contents lists available at ScienceDirect

Chemical Engineering Journal

journal homepage: www.elsevier.com/locate/cej

From single crystals to supported nanoparticles in oscillatory behavior of $CO + O_2$ reaction on platinum and palladium surfaces: Experiment and stochastic models

Vladimir I. Elokhin[a,b,*], Andrei V. Matveev[a,b], Evgenii V. Kovalyov[a], Vladimir V. Gorodetskii[a]

[a] Boreskov Institute of Catalysis SB RAS, Prosp. Akad. Lavrentieva 5, 630090 Novosibirsk, Russia
[b] Novosibirsk State University, 630090 Novosibirsk, Russia

ARTICLE INFO

Article history:
Received 6 December 2008
Received in revised form 16 April 2009
Accepted 17 April 2009

Keywords:
CO oxidation
Platinum
Palladium
Chemical waves
Nanoparticles
Carbon monoxide spillover
Monte Carlo model

ABSTRACT

The dynamic behavior of the catalytic CO oxidation reaction on the metal surfaces (Pt, Pd) of different structures (single crystals Pt(1 0 0), Pd(1 1 0); microcrystals (Pt, Pd tips); nanoparticles (Pd/support)) has been studied experimentally by FEM, HREELS, TPR, TDS, MB techniques and kinetic Monte Carlo modeling. The CO, O_2 adsorption and $CO + O_2$ reaction was studied by HREELS, TPR and TDS. Sharp tips of Pt and Pd, several hundreds angstroms in radius, were used to perform *in situ* investigations of the dynamic surface processes by FEM. HREELS studies on the Pt(1 0 0) surface demonstrate that the self-oscillations and waves propagation are connected with periodic changes in the surface structure of nanoplane (1 0 0)–(hex) $\leftrightarrow (1 \times 1)$, varying the catalytic property of metal. The fundamentally different feedback mechanism generating the kinetic oscillations has been identified on the Pd surfaces: the reversible subsurface oxygen formation, which modifies the adsorption and catalytic properties of the surface. Based on experimental results, two models for the $CO + O_2$ reaction on Pt(1 0 0) and Pd(1 1 0) surfaces are proposed for stochastic Monte Carlo modeling. Carbon monoxide spillover was taken into account in the stochastic model of oscillatory CO oxidation reaction over model Pd supported nanoparticles. The presence of CO_{ads} spillover determines the character of concentration waves over the Pd nanoparticle surface—oxygen wave propagates from the central particle part to the particle/support perimeter;—carbon monoxide wave moves in the opposite direction. The comprehensive study of CO, O_2 adsorption and $CO + O_2$ reaction in a row: single crystals → tips → nanoparticles have shown an identical nature of active centres over these metal surfaces.

1. Introduction

The catalytic oxidation of CO over platinum group metals exhibits a rich kinetic behavior, including regimes with sustained kinetic oscillations, for reviews see [1–3]. The kinetics of the reaction and the intermediates character on the Pt and Pd surfaces has been studied with the techniques of high-resolution electron energy loss spectroscopy (HREELS) [4], scanning tunneling microscopy (STM) [5], temperature-programmed reaction (TPR) [4,6] and molecular beam (MB) [7]. It has been found previously that the mechanisms of oscillatory CO oxidation are connected with a periodic change in surface structure Pt(1 0 0): hex $\leftrightarrow (1 \times 1)$ and with subsurface oxygen formation on Pd(1 1 0): $O_{ads} \leftrightarrow O_{sub}$ [1–3]. A common feature in all these mechanisms is the spontaneous periodical transitions of the metal surface from inactive to highly active states. Since the first discovery of a relationship between reconstruction and kinetic oscillations in CO oxidation on Pt(1 0 0) by Ertl [1], this has become one of the most extensively investigated oscillatory systems in heterogeneous catalysis. The use of spatially resolved (~1 μm) photoemission electron microscopy (PEEM) made it then possible to discover the formation of chemical waves on the Pt and Pd single crystal surfaces [1,2].

It is known that the supported catalysts are composed of active nano-sized metal particles exposing various nanoplanes. Recently, we have started to perform field electron microscopy (FEM) experiments on a sharp tips (~1000 Å) that are in many cases only about one order of magnitude larger than nanoparticles size in a supported catalyst. Sharp tips have been used to carry out *in situ* investigations of real dynamic surface processes where different crystallographic nanoplanes of the tip with a lateral resolution of ~20 Å are simultaneously exposed to the reacting gas and for which it is possible to study the interaction and the coupling of adjacent nanoplanes [8,9]. Many of the oscillatory reactions seen on Pt- and Pd-tip surfaces are examples of interplay of the different nano-sized plain surfaces [9].

* Corresponding author at: Boreskov Institute of Catalysis SB RAS, Prosp. Akad. Lavrentieva 5, 630090 Novosibirsk, Russia. Tel.: +7 383 3269326; fax: +7 3832 3308056.
E-mail address: elokhin@catalysis.ru (V.I. Elokhin).

1385-8947/$ – see front matter © 2009 Elsevier B.V. All rights reserved.
doi:10.1016/j.cej.2009.04.046

It seems likely that the CO oxidation is an ideal reaction for the study of "spillover" CO_{ads} effects on the catalytic properties of supported catalysts [10]. "Spillover" process involves a diffusion of carbon monoxide molecules, generated *via* molecular adsorption of CO on the support surface (Al_2O_3), into the metal nanoparticles (Pd) of Pd/Al_2O_3 bifunctional catalyst. The overall kinetics of CO oxidation is quite complex and is still not fully understood, in particular because the participation of "spillover" CO_{ads}, produced by CO adsorption on support surface [10] need to be considered for this reaction.

The direct comparison of catalytic properties of nano-sized planes (supported Pd particles, ~100 Å), with those of sharp tips (~10^3 Å) and extended single crystal surfaces (~10^8 Å) gives the possibility to bridge the "*structure gap*" between single crystal and nanoparticle surfaces, and to establish the intrinsic interrelation of reaction mechanism of CO oxidation on these surfaces. In this work, we study the temporal oscillation behavior of CO oxidation over Pd and Pt surfaces. The CO, O_2 adsorption and the intermediate reactivity (O_{ads}, O_{sub} and CO_{ads}) were studied by HREELS, TPR, TDS, MB techniques on the Pt(1 0 0) and Pd(1 1 0) single crystal surfaces.

Sharp tips of Pd and Pt (FEM) were used to perform *in situ* investigations of dynamic surface processes (chemical waves). Statistical lattice models [11] describing the temporal oscillation behavior of the CO oxidation on Pt(1 0 0), Pd(1 1 0) and nano-size supported Pd particles will be developed and analyzed.

2. Experimental

2.1. Experimental techniques in HREELS, TPR and TDS

The HREELS, TPR, TDS and MB experiments were performed in an ultra-high vacuum (UHV) chamber with a base pressure below 10^{-10} mbar. The energy loss spectra were obtained at the specular direction by using a VG ADES 400 electron spectrometer, an electron energy of ~2.5 eV and an incident angle of ~35° with respect to the surface normal. The resolution of the elastically reflected electron beam was about 9–11 meV (~70–90 cm^{-1}). The TDS and TPR spectra were measured with a quadrupole mass spectrometer (QMS) by using a heating rate of 6–10 K s^{-1}. The crystal surfaces were exposed to CO (or O_2) molecular beam by using a capillary array dozer. The gas flux of intensity 0.1 ML s^{-1} was controlled by mass spectrometry. The cleaning procedure of the Pt(1 0 0) and Pd(1 1 0) surfaces included Ar^+ etching and annealing cycles in oxygen and in vacuum. The structures of the clean single crystal surfaces were confirmed by low energy electron diffraction (LEED). The temperature of the single crystals was measured by means of chromel/alumel thermocouples spotwelded to the sample, and could be controlled to within 1 K by using a heating power supply with a feedback loop. The reaction gases, CO and O_2, were of the highest purity available, and were always checked by a mass spectrometry before use. The experimental setup has been described in detail elsewhere [12].

2.2. Experimental techniques in FEM

Experiments with field electron microscopy were performed in a separate UHV system, which was used simultaneously as a flow catalytic reactor. Details of the tip preparation of sharp radius (~10^3 Å) have been given elsewhere: Pt [13], Pd [14]. Depending on tip-radius preparation, different crystallographic nanoplanes may have a linear dimension of 50–200 Å. The Pt surface was cleaned by field evaporation and characterized by FEM at a field of ~0.3 V/Å, tip radius r = 680 Å, applied voltage at V ~1 kV. In FEM experiments, a negative voltage V is applied to a metal tip. Electrons are emitted into vacuum from the tip by tunneling through a potential barrier at the surface by the applied field and then are accelerated towards a fluorescent screen. A single or double channel plates were used as an image amplifier of a small electron emission current (~0.1 nA), and a video camera with a time resolution of 40 ms recorded *in situ* the dynamic behaviour of the surface processes [13,14]. The field electron current measures local properties of a surface with a lateral resolution of ~20 Å and magnification of ~3×10^5. The *in situ* measurement of surface reactivity, which is combined with work function (WF) alterations, concerns different nanoplanes surfaces simultaneously. Electrostatic field effects at the $F \sim 0.3$ V/Å used during these investigations are low enough not to affect the surface chemistry studied [15]. The FEM was operated with low electron current (~0.1 nA) to minimize gas collisions. The temperature at the tip could be controlled to within 1 K and was measured by means of a chromel/alumel thermocouple spot-welded to the metal loop near the tip. The reaction gases CO and O_2 of highest purity were introduced and measured by QMS. The FEM image and total field electron current were continuously monitored during the catalytic reaction at O_2 (~10^{-3} mbar) and CO (~10^{-4} mbar) partial pressures. It was demonstrated that at a pressure of up to ~10^{-3} mbar, stable emission currents could be obtained and the sputtering processes seem to be completely negligible. The FEM experimental device has been described before [9,16].

3. Results and discussion

3.1. Platinum: reaction mechanism and the corresponding Monte Carlo model

The CO oxidation at the steady state conditions over platinum metals (Pt, Pd) proceeds *via* a Langmuir–Hinshelwood (L–H) reaction:

$$CO + * \leftrightarrow CO_{ads}; \quad (1)$$

$$O_2 + 2* \rightarrow 2O_{ads}; \quad (2)$$

$$CO_{ads} + O_{ads} \rightarrow CO_2 + 2*; \quad (3)$$

where CO_{ads}, O_{ads}, and * are the adsorbed CO, oxygen and unoccupied surface sites, respectively. The first step (1) describes the molecular adsorption of CO. Oxygen adsorption is dissociative, step (2). Oxygen desorption proceed usually at T > 600 K, therefore step (2) could be considered as irreversible in the temperature range of CO oxidation (300–600 K). The final step (3) of interaction between O_{ads} and CO_{ads} is accompanied by immediate desorption of CO_2 into gas and liberation of two adsorption centres.

3.1.1. Pt(1 0 0)

The clean Pt(1 0 0) surface shows two surface structures (hex) and (1 × 1) that exhibit dramatically different adsorption and catalytic properties. This circumstance has made it the recognized system for the catalytic investigations. It is known that the hexagonal reconstruction (hex) to unreconstruction (1 × 1) is removed at CO, H_2 or NO low temperature adsorption [17]. The reversible (hex) ↔ (1 × 1) phase transition is a driving force for oscillations of CO or H_2 oxidation by O_2, which are accompanied on the Pt(1 0 0) surface by the propagation of chemical waves [18,19].

The atomic density of the (1 × 1) surface is 1.28×10^{15} Pt atoms cm^{-2} [17]. This is approximately 25% lower than the atomic density of the (hex) phase (i.e., 1.61×10^{15} Pt atoms cm^{-2} [20]). This density difference results in significant mass transport of platinum atoms during the back-reconstruction. STM data demonstrate [5,20] that expelled platinum atoms form clusters with size of ~15–25 Å. The back-reconstruction starts as soon the CO coverage on the (hex) surface exceeds the critical values of approximately 0.05–0.1 ML (one monolayer [ML] is equal to the number of platinum atoms of the topmost layer of the unreconstructed Pt(1 0 0)–1 × 1 surface)

[21]. As a result, the formation of adsorbed islands of CO with (1×1) structure is observed. The local coverage inside the (1×1) islands is assumed to be 0.5 ML during growth of the islands [21]. The (hex) phase surrounds the islands and is nearly free from CO_{ads} molecules.

3.1.2. O_2 adsorption

According to HREELS data, the oxygen adsorption to 30 Langmuirs ($1\,L = 1.33 \times 10^{-6}$ mbar s) at 90 K on the reconstructed Pt(1 0 0)–(hex) surface results in formation of molecular peroxide O_{2ads}^{2-} state with bond axis parallel to the surface and characterized by ν(O–O) band at 940 cm^{-1} and ν(Pt–O_2) band at 380 cm^{-1} (Fig. 1a) [22]. TD-spectra obtained from O_{2ads} layer indicates that all oxygen desorbs molecularly at 150 K and, hence, the peroxide O_{2ads}^{2-} molecular species does not dissociate (Fig. 1b).

Based on the HREELS data (Fig. 1c) an adsorption of O_2 (30 L) on (1×1) at 90 K results in formation of peroxide O_{2ads}^{2-} molecular species with frequency ν(O–O) band at 940 cm^{-1} and ν(Pt–O_2) band at 380 cm^{-1}. Opposite to the (hex) surface, oxygen adsorption on (1×1) is accompanied by formation of atomic oxygen O_{ads} with frequency ν(Pt–O) band at 500 cm^{-1}. TD-spectra obtained from the low temperature ($O_{ads} + O_{2ads}$) layer show the formation of two O_2 desorption peaks at 140 and 720 K (Fig. 1d). The high temperature oxygen peak is seen due to recombination of O_{ads} oxygen atoms. The HREELS and TDS date indicate that oxygen is molecularly adsorbed on the (hex) and dissociative—on (1×1) at 90 K. This is evidenced by the low values of a weakly adsorbed state in the HREEL/TD spectra on (1×1) and the intensive values for the oxygen atomic state.

A non-reconstructed Pt(1 0 0)–1×1 surface was prepared using the technique reported by Bonzel et al. [23], which involves: (i) saturating the (hex) phase surface with NO at 300 K; (ii) heating of NO_{ads} to 470 K in order for NO dissociation and N_2 desorption; (iii) reacting of O_{ads} with H_2 and finally the thermal desorption of hydrogen layer *via* flashing up to 390 K. NO_{ads} layer (with ^{15}N isotope labeling) was prepared on the Pt(1 0 0)–(hex) surface at an exposure of 5 L, T = 300 K (Fig. 2a). The adsorption on the (hex) surface leads to removal of the reconstruction. The NO_{ads} layer on (1×1) reveals two ν(NO) stretching bands at 1620 and 1800 cm^{-1} and a low-frequency ν(Pt–NO) band at 370 cm^{-1}. The adsorption state with ν(NO) band at 1800 cm^{-1} is assumed to occupy adsites of another kind (defects) produced during the phase transition (hex) → (1×1). In the course of a back-reconstruction induced by NO or CO adsorption causes the excess Pt atoms to be ejected over the upper layer of the metal surface with the formation of a small clusters (Fig. 2A and B). Hence, the ν(NO) at 1800 cm^{-1} can serve as a spectral indicator of the structural transformation of the Pt(1 0 0)–(hex) surface. The clean Pt(1 0 0)–1×1 surface is characterized by corresponding HREEL spectrum (Fig. 2a). Oxygen adsorpion (30 L) on (1×1) at 300 K is accompanied by the formation of an oxygen adatom layer with ν(Pt–O) band vibration frequencies at 530, 680 and 920 cm^{-1}. The band at 530 cm^{-1} represents stretching of adsorbed atomic oxygen as a result of oxygen adsorption on the (1 0 0)–(1×1)-terrace sites. In agreement with O_2/Pt(3 2 1) [4], the bands at 680 and 920 cm^{-1} are intrinsic to atomic states of oxygen on the structural defects (presumably like steps or kinks). The band at 1620 cm^{-1} represents a ν(NO) stretching of NO_{ads} (NO adsorption from a residual gas).

3.1.3. $CO + O_2$ reaction

The CO oxidation has been studied by HREELS within $CO_{ads} + O_{ads}$ coadsorption layers formed by the subsequent adsorption of O_2 and CO (Fig. 2a). Exposure of the O_{ads}/Pt(1 0 0)–(1×1) surface to 10 L of CO at 90 K results in the appearance of three main loss peaks at 450, 1880 and 2100 cm^{-1}, attributed to the ν(Pt–CO) and the ν(CO) stretching modes of CO_{ads} molecules in the bridge and on-top states [12]. Fig. 2b shows a set of CO_2, CO and O_2 TPR spectra obtained from the resulting mixed $CO_{1\times1} + O_{1\times1}$ adlayers. We have found that interaction of atomic oxygen layer O_{ads} with CO_{ads} is accompanied by formation of four CO_2 peaks: at 140, 180, 260 and 310 K. The N_2 peak at 420 K represents decomposition of NO_{ads} molecules (impurities). Fig. 3a shows a set of CO_2, CO and O_2 TPR spectra of the mixed adlayers $CO_{ads} + O_{ads} + O_{2ads}$ on the Pt(1 0 0)–(1×1) surface. The characteristics of the initial oxygen layer ($O_{ads} + O_{2ads}$) are presented by HREELS and TDS spectra in Fig. 1c and d. From the result shown in Fig. 3a it may be concluded that molecular oxygen is inactive in the CO_2 formation—O_{2ads} layer desorption proceed at 140 K.

According to our early HREELS data [16], subsequent O_2 adsorption at 90 K on the reconstructed Pt(1 0 0)–(hex) surface precovered with the $CO_{1\times1}$ islands (1 L CO, 300 K, islands) results in the formation of molecular peroxide, O_{2ads}^{2-}, with a characteristic ν(O–O) band at 920 cm^{-1}. CO_2, CO and O_2 TPR spectra, obtained from the resulting mixed $CO_{1\times1} + O_{2ads}$ adlayers, indicates that O_{2ads} and CO_{ads} desorbs molecularly at 140 and 510 K, respectively, without any CO_2 formation (Fig. 3b). This observation supports the idea that the $CO_{1\times1}$ islands have a high local coverage (0.5 ML) [21], and therefore do not allow for the dissociation of the molecular oxygen O_{2ads}^{2-} inside these islands. The obtained results of HREELS/TDS studies revealed that two Pt(1 0 0) surface structures are distinct in their capacity to dissociate O_2: for the (1×1) phase the process occurs already at 90 K, while for the (hex) surface it requires some activation and will be limited by the low sticking coefficient of oxygen [5]. In combination with the formation of $CO_{1\times1}$ islands at 300 K on (hex), dissociation of the O_{2ads} is hindered.

It is known that CO adsorption on Pt(1 0 0)–(hex) at 90 K occurs in on-top sites without lifting of the reconstruction [21], and is characterized by ν(Pt–CO) and ν(CO) bands at 450 and 2120 cm^{-1}, respectively [16]. Exposure of this CO_{hex} pre-covered surface to 10 L of O_2 results in the formation of O_{2ads}^{2-} layer, characterized by the ν(O–O) band at 900 cm^{-1}. According to our early TPR data the heating of mixed $CO_{hex} + O_{2ads}^{2-}$ molecular adlayers leads to low temperature formation of significant amount of CO_2 that desorbed at 140, 190, 290 and 350 K, respectively, contrary to the case in Fig. 3b [16]. It is known that the hexagonal reconstruction can be removed at low temperatures (below ~200 K) by CO adsorption [24]. Hence, the $CO_{ads} + O_{ads} \rightarrow CO_{2\ gas}$ reaction in the low temperature region (below ~200 K) could be clarified by the formation of the islands of the (1×1) phase due to back-reconstructive CO adsorption, dissociation of the O_{2ads}^{2-}, adsorbed on the defect sites of the Pt(1 0 0)–(1×1), then the reaction in the mixed $CO_{hex} + O_{2ads}^{2-}$ molecular adlayers become possible [16].

3.1.4. FEM: Pt-tip experiments

The surface analysis of the Pt-tip by FEM is based on the fact that due to adsorption of CO and oxygen, local work function changes ($\Delta\varphi$) can be correlated with the total field electron current. The significant difference in WF values gives an excellent tool for distinguishing transition in the adsorption layers: the O_{ads} layer (dark regions) with low emission current and CO_{ads} layer (bright regions) with high emission current. Fig. 4B demonstrates the example of the appearance of a sharp boundary between the mobile CO_{ads} (grey) and O_{ads} (black) fronts in the $CO + O_2$ oscillatory reaction on the Pt-tip surface.

Fig. 4A represents a typical series of oscillations of electron current when the Pt-tip with [1 0 0]-orientation is exposed at 365 K to a gas reaction mixture of $P(O_2) = 5 \times 10^{-4}$ mbar and $P_{(CO)} = 8 \times 10^{-6}$ mbar. The oscillation amplitude ranges from the O_{ads} layer (low current) to the CO_{ads} layer (high current). A difference of WF values between O_{ads} and CO_{ads} of ~0.4 eV is connected with a change in the electron current. One short cycle (8 s) of oscillations is illustrated in Fig. 4A. Since the WF increased due

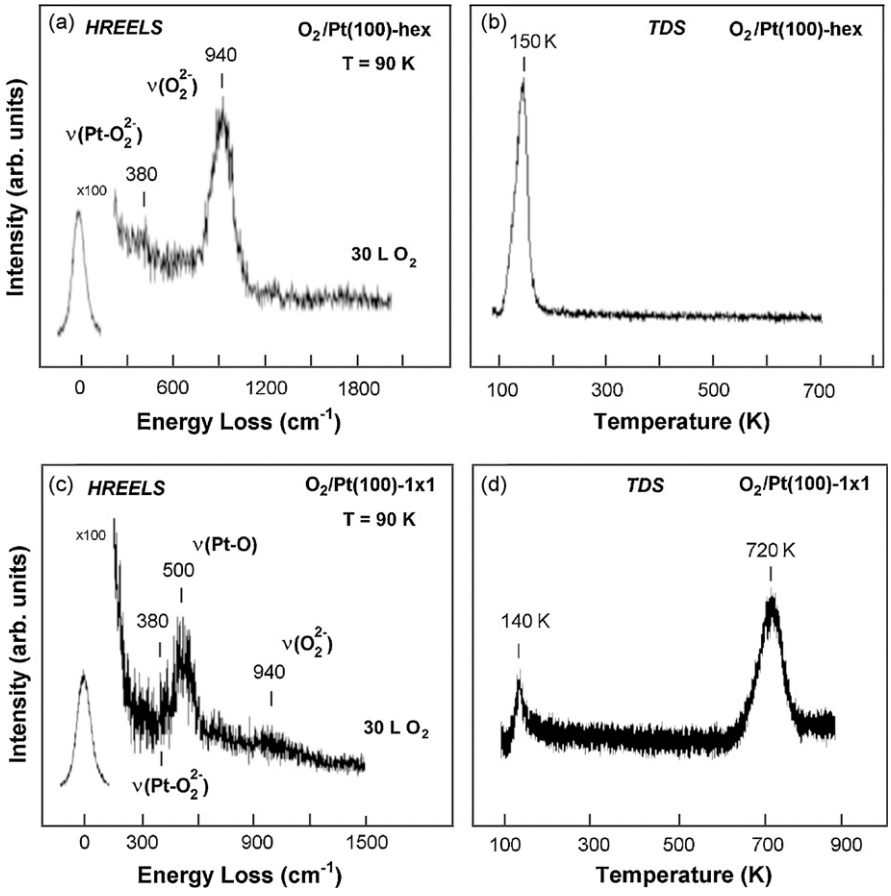

Fig. 1. (a) HREEL spectrum obtained after 30 L O_2 exposure on the Pt(1 0 0)–(hex) surface at 90 K. (b) TD spectrum from the adsorbed molecular oxygen prepared in (a). (c) HREEL spectrum obtained after 30 L O_2 exposure on the Pt(1 0 0)–(1 × 1) surface at 90 K and (d) resulting TD spectrum obtained after oxygen adsorption prepared in (c).

to chemisorbed oxygen layer ($\Delta\varphi$ = 1.1 eV) is higher than that of the CO_{ads} layer ($\Delta\varphi$ = 0.7 eV) [13], the relative surface brightness is (black) for O_{ads}, (grey) for CO_{ads} and (white) for unoccupied clean surface sites. The sequence of images in Fig. 4B corresponds to the following steps of CO + O_2 reaction: (a) at τ = 0 s: O_{ads} layer is present on the (1 0 0), (3 1 0), (2 1 0) and (1 1 0) planes (black); CO_{ads} layer is present on the (1 1 1), (1 1 2), (1 1 3) planes and their surrounding (grey); (b) at τ = 2 s: (1 1 3), (3 1 0) planes are mainly covered by CO (grey), while the unreconstructed Pt(1 0 0)–(1 × 1) nanoplane is completely covered with a O_{ads} island (shown as a (black) patch); (c) at τ = 4.1 s: a very fast catalytic surface process (the "clean-off" CO_{ads} + O_{ads} reaction) removes the O_{ads} layer. At this point the clean

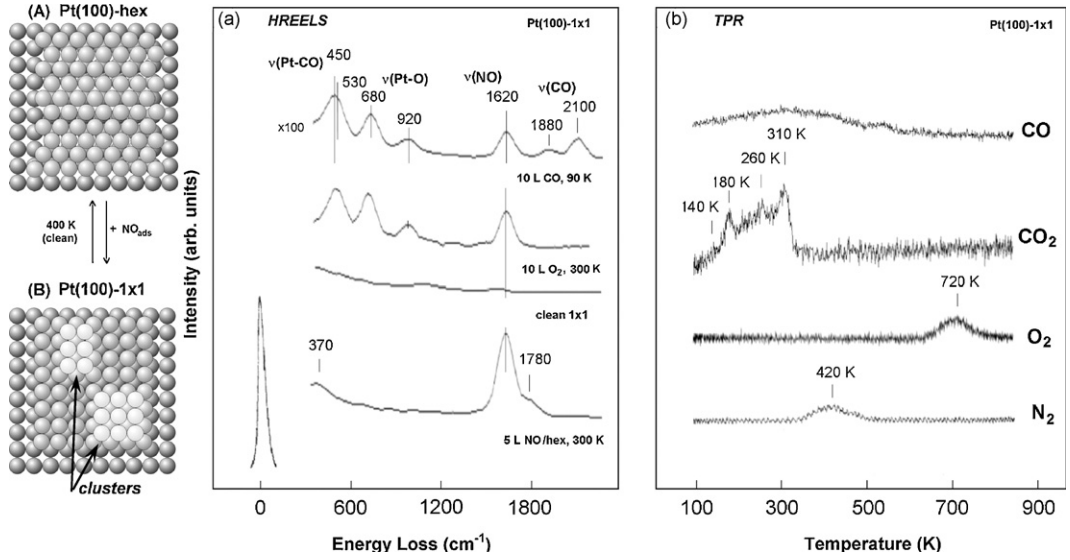

Fig. 2. Plan view of the Pt(1 0 0) single crystal shows the atomic structure on the reconstructed (1 0 0)–(hex) (A) and unreconstructed (1 0 0)–(1 × 1) (B) surfaces. (a) HREEL spectra obtained after O_2 exposure of a 10 L at 300 K on a Pt(1 0 0)–(1 × 1) surface (prepared by the method proposed by Bonzel et al. [23]) and subsequent carbon monoxide adsorption after an exposure of a 10 L CO at 90 K. (b) TPR spectra from the coadsorbed atomic oxygen and carbon monoxide layer prepared in (a).

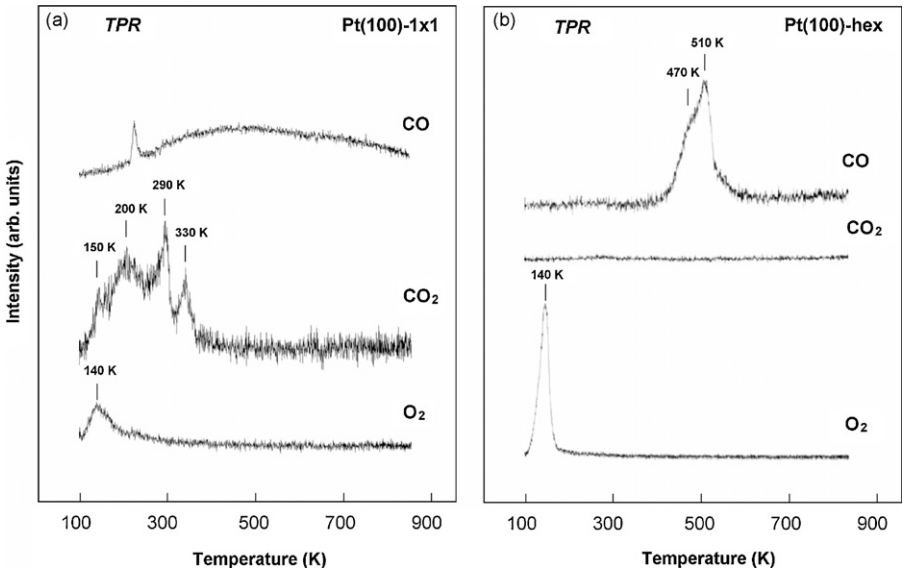

Fig. 3. (a) TPR spectra from the coadsorbed (atomic + molecular) oxygen states obtained after O_2 exposure of a 30 L at 90 K on a Pt(1 0 0)–(1 × 1) surface and subsequent carbon monoxide adsorption after an exposure of a 10 L CO adsorption at 90 K. (b) TPR spectra from the coadsorbed molecular oxygen and carbon monoxide layers obtained after O_2 exposure of a 10 L at 90 K on a Pt(1 0 0)–(hex) surface pre-covered by CO_{ads}/(1 × 1) islands after CO exposure (1 L) at 300 K.

unstable (1 × 1) surface suddenly reconstructs to the (hex) structure, creating an unoccupied clean (1 0 0) surface (white); (d) at τ = 4.5 s: the small sticking coefficient for oxygen on this surface, 10^{-3}, keeps this reconstructed plane free from O_{ads} layer until, at a certain local CO_{ads} coverage, the reconstruction is lifted again, and the (1 × 1) structure is returned (grey); (e) at τ = 7.0 s: the increase in oxygen sticking coefficient from $S_0 \sim 10^{-3}$ (hex) to $\sim 10^{-1}$ (1 × 1) is accompanied by the appearance of O_{ads} island (black); (f) at τ = 8.0 s: the cycle time lasts when the oxygen reaction with CO_{ads} starts again, forming a wave (O_{ads}) with a sharp boundary moving from (1 0 0) plane towards the {3 1 0}, {2 1 0}, {1 1 0} planes as result of the transition from a catalytically inactive state into an active surface for CO oxidation.

Details of the oscillatory behavior depend sensitively on the external control parameters, i.e. the selected temperature and partial pressures [25]. For T = 340 K, as an example, the kinetic phase diagram has been established for the Pt(1 0 0) nanoplanes (~200 Å dimension) on a Pt-tip [16]. This diagram compared well with that for a Pt(1 0 0) single crystal surface over a much higher (440–520 K) temperature range [26]. It is shown that the values of wave front propagation rates measured by FEM studies have the same order of magnitude as those measured by PEEM [13].

3.1.5. Pt: modeling of oscillations and wave patterns

Our FEM results have surprisingly shown very sharp reaction fronts, therefore the nature of the *local reaction rates* are of great chemical interest. Actual mechanism describing such a sharp reaction zone formation are based on a local transformation of the Pt(1 0 0)–(hex) ↔ (1 × 1) and the appearance of certain concentration of empty sites. HREELS and TPR results have strongly suggested that the CO-induced (hex) → (1 × 1) phase transition observed on Pt(1 0 0) single crystal is the driving force for the isothermal oscillations seen on that surface. The oscillation cycles of the CO oxidation on Pt(1 0 0) surface has been explained by Imbihl et al. [27,28].

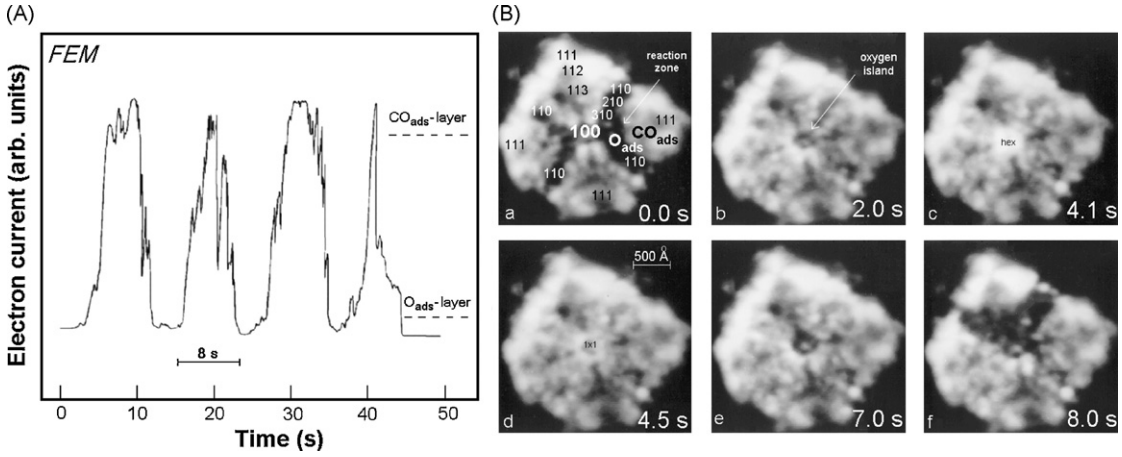

Fig. 4. (A) Oscillatory behaviour of the total field electron current for the Pt-tip at constant control parameters: T = 365 K, $P_{(CO)} = 8 \times 10^{-6}$ mbar, $P_{(O_2)} = 5 \times 10^{-4}$ mbar. Low current levels reflect O_{ads}-covered planes (except {1 1 1} and surroundings $\{1\,1\,1\}_{st}$ planes, which remain CO_{ads}-covered). $F \approx 0.4$ V/Å. (B) Sequence of FEM images showing the surface activity of different crystallographic nanoplanes. (a) Stereographic projection of a Pt[1 0 0]-oriented tip; at τ = 0 s, the (1 0 0) plane and the {1 1 0} vicinals temporary covered by oxygen O_{ads} layer. (b) After τ = 2 s, the O_{ads} layer shrinks due to a slow reaction and locates on the (1 0 0)–(1 × 1) surface. (c) After τ = 4.1 s, a very bright image indicates a clean (1 0 0) surface (hex-reconstructed). (d) τ = 4.5 s, a small CO_{ads} coverage forms and the reconstruction is lifted ((hex) → (1 × 1)). (e) τ = 7.0 s, the restoration of the O_{ads} island on the (1 0 0)–(1 × 1) surface. (f) τ = 8.0 s, the reconstruction of the O_{ads} layer to (a).

According to the reaction model [28], the mechanism for CO oxidation over nanoplane (1×1) of the Pt-tip surface has the following key stages:

(i) On a starting (hex) surface (CO-side of reaction), the low value of the oxygen-sticking coefficient ($S_0 \approx 10^{-3}$) results in preferential adsorption of CO ($S_0 \approx 0.8$) from the gas mixture (Fig. 4B(c)). When the CO_{ads} coverage approaches the value ~0.08 ML, the (hex) → (1×1) phase transition is initiated (Fig. 4B(d)), and islands with $CO_{1\times1}$ structure grows at the expense of the (hex) surface area.

(ii) According to HREELS data [16], the local $CO_{1\times1}$ (0.5 ML) layers and the (hex) surface areas both inhibit O_2 dissociative adsorption and the $CO_{1\times1} + O_{2ads}$ reaction (Fig. 3b). On the other hand, the generation of empty sites as a result of the $CO_{hex} \rightarrow CO_{1\times1}$ phase transition [7] permits O_2 dissociation with O_{ads} layer formation [16]. A fast reaction between these O_{ads} atoms and CO_{ads} (Fig. 3a), and the creation of vacant surface sites for fast oxygen adsorption leads to an autocatalytic CO_2 formation step. The $CO_{1\times1}$ coverage then decreases, and an O_{ads} layer on the (1 0 0) plane is formed (Fig. 4B(e and f)).

(iii) The areas, where CO molecules are consumed, are replenished either by CO molecules from the gas phase or by surface diffusion from the adjacent areas, where CO_{ads} layers are still present (Fig. 4B(a and b)). The reduced local oxygen coverage by "clean-off" reaction destabilizes the (1×1) phase and leads to the transformation to the (hex) phase (Fig. 4B(c)), until the initial state (i) is reached again.

The detailed mechanism of the CO oxidation process is given in Scheme 1 [29] .

(1) CO adsorption: the absence of indices near the centre * implies that CO, unlike oxygen, is considered to have equal sticking probability on both $*_{hex}$ and $*_{1\times1}$. The rate coefficient for CO adsorption ($k_1 = 3.9 \times 10^5$ ML s^{-1} mbar^{-1}) was adopted from Ref. [27,Table 1]. (2) and (3) CO desorption: the rate coefficients for CO desorption on (hex) and (1×1) phases differ widely (approximately by three-four orders of magnitude). In our simulations $k_2 = 4\ s^{-1}$, $k_3 = 0.03\ s^{-1}$ [27]. (4) Structural phase transformation (hex) → (1×1). In accordance with [7] let us assume that CO_{ads} (both CO_{hex} and $CO_{1\times1}$) adsorbed on four (2×2) neighboring centres of the lattice would transform these centres (with some probability) into the (1×1) structure. In our simulations $k_4 = 3\ s^{-1}$. (5) Back structural phase transition (1×1) → (hex). Value of $k_5 = 2\ s^{-1}$ at $T \sim 500$ K was taken from [27]. (6) Oxygen adsorption: O_2 molecules adsorbs dissociative only on the two neighboring (1×1) centres, $k_6 = 7.4 \times 10^5$ ML s^{-1} mbar^{-1} [27]. (7) CO_2 formation: the surface reaction proceeds *via* the L–H mechanism conserving the type of the active centres. Adsorbed oxygen interacts equally with both CO_{hex} and $CO_{1\times1}$. We assume that the rate of CO_2 formation is very high: therefore in our MC-model the reaction proceeds immediately when O_{ads} and CO_{ads} appear as the nearest neighbors. (8) CO diffusion: CO_{ads} molecules can diffuse *via* hopping from their sites to vacant nearest neighbor site and the type of active centres remains the same. Along with the stage (7) this process offers an additional source of empty active centres $*_{1\times1}$ required for dissociative oxygen adsorption. Monte Carlo simulations on Pt(1 0 0) could reproduce both the oscillations of the rate of CO_2 formation and the appearance of surface waves [29].

1) $CO + * \rightarrow CO_{ads}$ (CO_{hex} or $CO_{1\times1}$)

2) $CO_{hex} \rightarrow CO + *_{hex}$

3) $CO_{1\times1} \rightarrow CO + *_{1\times1}$

4) (hex) → (1×1): $4\ CO_{ads} \rightarrow 4\ CO_{1\times1}$

5) (1×1) → (hex): $*_{1\times1} \rightarrow *_{hex}$

6) $O_2 + 2*_{1\times1} \rightarrow 2O_{1\times1}$

7) $O_{1\times1} + CO_{ads} \rightarrow CO_2 + *_{1\times1} + *$

8) $CO_{ads} + * \rightarrow * + CO_{ads}$

Scheme 1.

We used in modeling a square $N \times N$ lattice with the periodical boundary conditions, imitating the metal surface. The states of lattice cells were set according to the rules determined by the detailed mechanism of the reaction. The time was measured in terms of the so-called Monte Carlo steps (MC step) consisting of $N \times N$ trials to choose and realize the elementary processes. For one MC step, each cell was called once in the average. The probability of each step for the processes of adsorption, desorption and reaction was determined by the ratio of the rate constant of a selected elementary step to the sum of the rate constants of all steps.

After each choice of one of the processes and an attempt to realize it, the program considered the internal diffusion cycle that involved M diffusion attempts for CO_{ads} molecules (usually $M = 50$–100). The reaction rate of CO oxidation and the surface coverages ($\theta(O_{ads})$, $\theta(CO_{ads})$, $CO_{ads} = CO_{hex} + CO_{1\times1}$, and the fraction of (1×1) surface, $\theta(1 \times 1)$) were calculated after each MC step as a ratio of the amount of CO_2 molecules formed (or the number of lattice cells in the corresponding state) to the overall amount of cells N^2 (the procedure was described in [29]).

Fig. 5 shows self-oscillations of the rate of CO_2 formation, the surface coverages with O_{ads} and CO_{ads}, and the fraction of (1×1) surface. At the initial moment, the (1 0 0) surface is in the (hex) structure and only CO adsorption is allowed. Despite the low rate of (hex) → (1×1) transition, the fraction of (1×1) surface rapidly grows. The value of $O_{1\times1}$ coverage is very low due to the fast reaction with neighboring CO_{ads} molecules. When the maximal value of $\theta(CO_{ads})$ ~0.8 is attained, the adsorbed layer largely consists of CO_{hex} and $CO_{1\times1}$ (Fig. 6A). Fig. 6a shows that the rate of CO_2 formation inside the CO_{ads} layer is low, but regions with an enhanced concentration of vacant sites are available on the surface. In these regions, the $O_{1\times1}$ islands nucleate and propagate along the metal surface (Fig. 6B and C). Fig. 6b and c show that the maximal intensity of CO_2 molecule formation is observed in the narrow zone at the boundary of growing O_{ads} island inside of CO_{ads} layer. The appearance of such a narrow reaction zone with the maximum intensity of CO_2 formation (wave front) was experimentally observed by the field ion probe-hole microscopy technique with a resolution of ~5 Å [16]. The rate of CO_2 formation has an intermediate value inside the $O_{1\times1}$ island and the lower rate—inside the $CO_{1\times1}$ layer. The highest

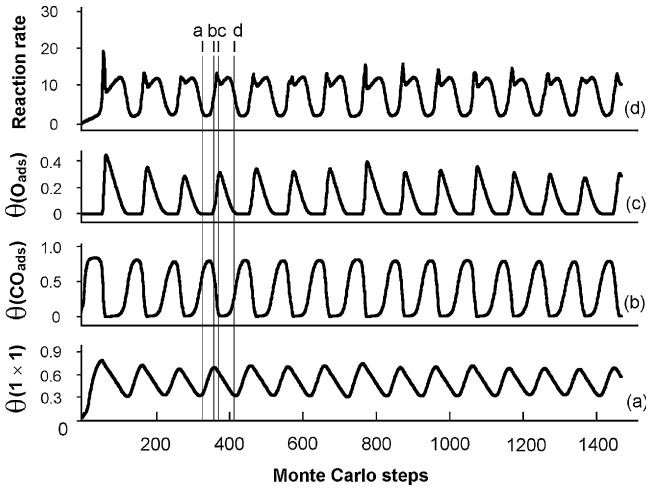

Fig. 5. Oscillations of the reaction rate and the surface coverage (θ) of Pt(1 0 0) for the lattice size $N = 384$ and the parameter $M = 100$. The values of the rate constants of elementary steps (Scheme 1) $k_1 = 3.9 \times 10^5$ ML s^{-1} mbar^{-1}, $P_{CO} = 6.6 \times 10^{-5}$ mbar, $k_2 = 4\ c^{-1}$, $k_3 = 0.03\ c^{-1}$, $k_4 = 3\ c^{-1}$, $k_5 = 2\ c^{-1}$, $k_6 = 7.4 \times 10^5$ ML s^{-1} mbar^{-1}, $P_{O_2} = 1.3 \times 10^{-4}$ mbar, k_7 = infinity (see text).

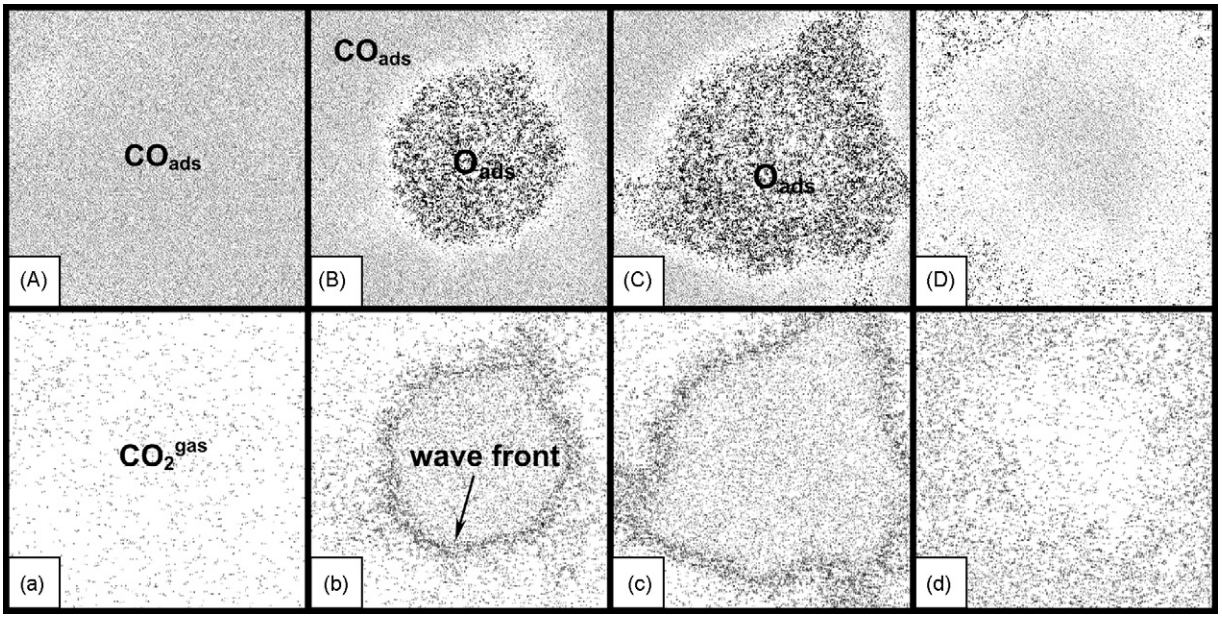

Fig. 6. The distribution of adsorbates over the surface (A–D) and the intensity of CO_2 formation (a–d) at the moment when the surface coverages changes on Pt(1 0 0). The concentration of O_{ads} is shown in black, CO_{ads} is in grey, and free surface is in white. Snapshots A–D, a–d correspond to the moments a–d shown with the bars in Fig. 5.

value of the reaction rate along the oscillation period corresponds to the point when the perimeter of the reaction zone has a maximum length (Fig. 6c). At the end of the oscillation cycle, the $\theta(O_{ads})$ coverage decreases due to CO + O reaction with the subsequent transition of the (1×1) phase into (hex) (Fig. 6D and d).

3.2. Palladium: reaction mechanism and the corresponding Monte Carlo model

Contrary to Pt(1 0 0), the clean Pd(1 1 0) surface does not demonstrate the reversible surface phase transitions during catalytic CO oxidation. The oscillations in the reaction rate are associated with changes in oxygen adsorption probabilities (S_0) induced by formation and depletion of subsurface oxygen: $O_{ads} \leftrightarrow O_{sub}$ [1,2].

According to our TDS data [30], oxygen adsorption on the Pd(1 1 0) surface at 100 K results in the formation of molecular and atomic states. Above a 0.3 L exposure, there are three peaks in the spectrum, around 125 (α-O_2 molecular state), 740 (β_1-O atomic state), and 815 (β_2-O atomic state) K. The β_1-oxygen state has been attributed to subsurface oxygen ($O_{ads} + {}^*_v \rightarrow {}^*O_{sub}$, here $^*_v$ are the active sites in the subsurface layers), as indirectly indicated by XPS [30] and WF measurements [31]. CO adsorption (50 L) at 100 K on the clean Pd(1 1 0) surface leads to several molecular CO_{ads} states with desorption peak temperatures at 230 (α_1), 280 (α_2), 330 (α_3) K, and higher temperature features at 410 (β_1) and 470 (β_2) K [30].

The effect of subsurface oxygen on the rate of the $CO + O_{ads} \rightarrow CO_2$ reaction was studied by TPR experiments [32]. It has become clear that the differentiation between adsorbed (O_{ads}) and subsurface (O_{sub}) oxygen is difficult. An attempt has been made in our studies to investigate the activity of the subsurface oxygen towards CO by using ^{18}O labeling.

Fig. 7 shows the isothermal desorption spectra (Iso-TDS) for cases where the clean Pd(1 1 0)–(1×1) surface (A) was first exposed to 0.2 L of $^{18}O_2$ at 100 K and then preheated to 500 K to produce a ^{18}O/Pd(1 1 0)–(1×2) reconstructed surface (B). This was followed by adsorption of 0.8 L of $^{16}O_2$ at 100 K and preheating to up to 200 K (to desorb any molecular $^{16}O_{2ads}$). This procedure was designed to prepare a Pd(1 1 0) surface with a $^{16}O_{ads}$ layer on top of $^{18}O_{sub}$ subsurface oxygen. The reconstruction of the surface from its (1×1) phase to a (1×2) structure facilitates the formation of the O_{sub} species, because on the (1×2) reconstructed surface approximately 50% of the surface sites are located below the uppermost Pd atoms, and that makes the diffusion of oxygen ($^{18}O_{ads}$) into the subsurface region easier. Iso-TD spectra have been received with the molecular beam of CO (Fig. 7C). Starting from time $\tau = 0$, the surface was exposed to a $C^{16}O$ molecular beam of intensity 0.1 ML s^{-1} and competitive reactions: (i) the yield of carbon dioxide formed by the reaction of CO with adsorbed atomic oxygen, $^{16}O_{ads} + C^{16}O \rightarrow C^{16}O^{16}O + C^{16}O_{ads}$ (upper curves in Fig. 7C), and (ii) with subsurface atomic oxygen, $^{18}O_{sub} + C^{16}O \rightarrow C^{16}O^{18}O + C^{16}O_{ads}$ (lower curves in Fig. 7C), were recorded. As can be seen, at $T \sim 230$–300 K, $^{18}O_{sub}$, oxygen atoms incorporated into the subsurface layer of the palladium react with CO much more slowly compared to $^{16}O_{ads}$. This result clearly shows that the reactivity of O_{ads} is higher than that of O_{sub} oxygen.

3.2.1. PEEM and FEM experiments

The $CO + O_2$ reaction on the Pd(1 1 0) single crystal and Pd-tip surfaces were investigated using the PEEM, FEM, MB techniques to learn the details of the reaction dynamics [30,32,33]. At 300 K the reaction is limited by oxygen adsorption because the surface is covered with CO_{ads}. In the temperature interval between 370 and 450 K the rate for CO_2 production increases rapidly due to CO_{ads} desorption. Moreover, in this temperature region the hysteresis (bistability) in CO_2 formation rate had been observed in experiments with rise and decrease of the temperature. As the temperature is increased, the transfer from the CO_{ads} layer into the O_{ads} layer is delayed, while when the temperature is decreased, the reverse is true. An example of the oscillations in CO_2 production over Pd(1 1 0) surface ($T = 390$ K, $P_{O_2} = 5 \times 10^{-2}$ mbar, $P_{CO} = 5 \times 10^{-5}$ mbar) was reported earlier [30]. The formation of a spatial-temporal pattern of oxygen- or CO-adsorption layers occurs under the same conditions of bistability (P_i, T). An example for the formation of spiral waves is shown in Fig. 8A [33]. At the Pd(1 1 0) surface the CO adsorption creates a higher WF ($\Delta\varphi = 1.05$ eV) than the adsorption of oxygen ($\Delta\varphi = 0.75$ eV). In Fig. 8A, therefore, the dark regions characterize CO_{ads} layers. The crystallographic orientation indicates the anisotropy of the spatio-temporal adsorption structures (along the rows of metal atoms in [1 $\bar{1}$ 0]-direction) displayed with a 380 μm image diameter. The dynamics of a spiral

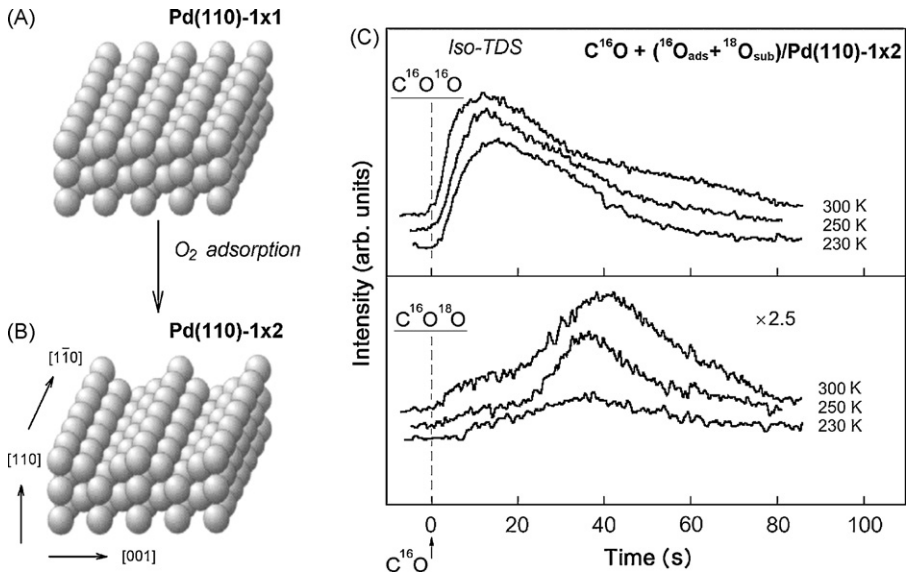

Fig. 7. Plan view of the Pd(1 1 0) single crystal shows the atomic structure on the unreconstructed (1 1 0)–(1 × 1) (A) and reconstructed (1 1 0)–(1 × 2) (B) surfaces. Isothermal desorption spectra shows the rate of CO_2 formation with time during the titration of a mixed oxygen layer composed of adsorbed $^{16}O_{ads}$ and subsurface $^{18}O_{sub}$ atomic oxygen with a $C^{16}O$ molecular beam of intensity 0.1 ML s^{-1} starting from $\tau = 0$. The reaction rate was measured at 230, 250, and 300 K. The upper and lower spectra refer to the reactions $^{16}O_{ads} + C^{16}O \rightarrow C^{16}O^{16}O + C^{16}O_{ads}$ and $^{18}O_{sub} + C^{16}O \rightarrow C^{16}O^{18}O + C^{16}O_{ads}$, respectively.

wave is visualized at resulting time images (τ = 0–0.6 s) (Fig. 8A). The qualitative explanation for a spiral wave rotation was attributed to anisotropic surface diffusion of CO being fast along the rows of metal atoms on (1 1 0), and slow—perpendicular to the rows (Fig. 7A and B).

Isothermal, non-linear dynamic processes for the CO + O_2 reaction on Pd-tips, as well as the formation of face-specific adsorption islands and the mobility of reaction/diffusion fronts, were studied by FEM [30]. The initiating role of Pd {1 1 0} nanoplanes for the generation of local waves on the Pd-tip surface was established. Fig. 8B shows the series of FEM oscillations detected, when the Pd-tip was exposed to a CO + O_2 reaction mixture at 425 K. The oscillation amplitude obtained when going from CO_{ads} (low current) to O_{ads} (high current) layers has a periodicity of ~5 s. A difference in WF between the CO_{ads} and O_{ads} covered surfaces of ~0.6 eV is connected with these electron current intensity changes. Analysis of the Pd-tip surface with a local resolution of ~20 Å shows the availability of a sharp boundary between the mobile CO_{ads} and O_{ads} fronts. The O_{ads} and CO_{ads} layers interacts *via* a sequence of reaction steps, including a reversible $O_{ads} \leftrightarrow O_{sub}$ transition, which acts as the feedback step during the oscillations, to cause the chemical waves.

3.2.2. Pd: modeling of oscillations and wave patterns

The catalytic oxidation of CO over Pd(1 1 0) surface exhibits temporal oscillations under a certain range of reaction parameters: T and P_i. A feedback mechanism for oscillations is associated with the changes in the sticking probability of oxygen (S_0) induced by formation and depletion of subsurface oxygen (Pd(1 1 0): $O_{ads} \leftrightarrow O_{sub}$). The model [3] assumes that the O_{sub} layer simultaneously blocks oxygen adsorption and helps the growth of CO_{ads} layers, leading to surface reaction poisoning (low rate of CO_2 formation). A slow CO_{ads} reaction with O_{sub} removes the subsurface oxygen, after which O_2 adsorption become possible (high rate of CO_2 formation). Then, the subsurface oxygen layer forms again and the cycle is restored. Based on our TPR, PEEM, MB and FEM data regarding CO oxidation over

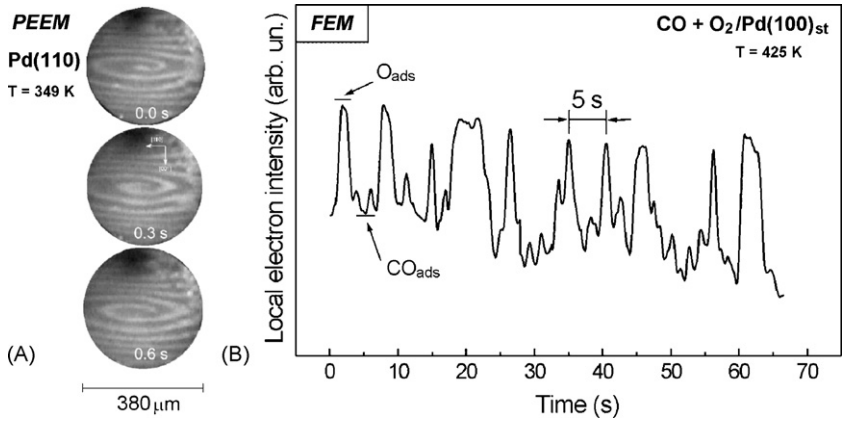

Fig. 8. (A) Dynamics of PEEM images of the surface in the case of existence of a spiral wave in CO oxidation on Pd(1 1 0) [33]: $P_{O_2} = 5.3 \times 10^{-3}$ mbar, $P_{CO} = 2.1 \times 10^{-5}$ mbar, T = 349 K. Dark regions shows CO_{ads}, light regions, O_{ads} layers. (B) Variations in local emission current from a Pd(1 0 0)$_{step}$ plane as a function of time during an oscillatory reaction between CO and O_2 on a Pd-tip under constant reaction conditions, T = 425 K, $P_{O_2} = 2.6 \times 10^{-3}$ mbar, and $P_{CO} = 1.3 \times 10^{-4}$ mbar. Low current levels reflects a Pd(1 0 0) nanoplane covered by CO_{ads}.

Atomic oxygen route

1) $O_2 + 2^* \rightarrow 2O_{ads}$

2) $CO + {}^* \leftrightarrow CO_{ads}$

3) $CO_{ads} + O_{ads} \rightarrow CO_2 + 2^*$

Subsurface oxygen route

4) $O_{ads} + {}^*_v \rightarrow {}^*O_{sub}$

5) $CO_{ads} + {}^*O_{sub} \rightarrow CO_2 + 2^* + {}^*_v$

6) $CO + {}^*O_{sub} \leftrightarrow CO_{ads}/O_{sub}$

7) $CO_{ads}/O_{sub} \rightarrow CO_2 + {}^* + {}^*_v$

Scheme 2.

Pd surfaces [9,30,32–34], some elementary steps have been added to the classic L–H scheme, namely in Scheme 2.

Here * and $^*_v$ are the active sites on the clean surface and subsurface layers, respectively. The 1st step describes irreversible oxygen adsorption; the 2nd step is the adsorption and desorption of CO. The 3rd step corresponds to the reaction between CO_{ads} and O_{ads}. Formation of the subsurface oxygen proceeds according to step (4). The reaction between the nearest neighbor CO_{ads} and O_{sub} is described by step (5). The formation of a CO_{ads}/O_{sub} intermediates occurs both *via* the direct adsorption of CO from the gas (step 6), and *via* CO_{ads} diffusion along the surface. The CO_{ads}/O_{sub} decomposition is accompanied by the formation of CO_2 molecules and appearance of empty sites: * and $^*_v$ (step 7). We suppose that the heat of CO adsorption on the subsurface centres [$^*O_{sub}$] is less than that on the initial * one. Also it was assumed that the probability of carbon monoxide desorption from CO_{ads}/O_{sub} species (step 6) is higher than that of CO_{ads} (step 2) one. The CO_{ads} molecules can diffuse over the surface according to the following rules: (i) $CO_{ads} + {}^* \leftrightarrow {}^* + CO_{ads}$, (ii) $CO_{ads} + {}^*O_{sub} \leftrightarrow {}^* + CO_{ads}/O_{sub}$, (iii) $CO_{ads}/O_{sub} + {}^*O_{sub} \leftrightarrow {}^*O_{sub} + CO_{ads}/O_{sub}$. The sequence of steps (1–5) is often used for modeling of oscillations in CO oxidation on the platinum metals including the Monte Carlo models. In our study, in addition to steps (1–5), the possible process of CO_{ads}/O_{sub} intermediate sites formation has been considered both due to CO adsorption (step 6), and to the CO_{ads} diffusion over the surface. Step (4) is supposed to be irreversible.

The following sequence of the certain elementary reaction steps for an oscillatory cycle has been proposed: (i) O_{sub} forms only on the O_{ads} covered surface that accompanied by a fast decrease of S_0 for the O_2 adsorption; (ii) CO_{ads} layer formation is a result of the fast reaction of carbon monoxide molecules with O_{ads} layer; (iii) the enhanced concentration of the empty sites appears due to slow $CO_{ads} + O_{sub}$ reaction to form CO_2; (iv) the transfer of surface from the lowest activity (O_{sub} layer) to the high level (O_{ads} layer) occurs simultaneously both *via* the increase of S_0 for the O_2 adsorption and *via* the decrease of O_{sub} concentration.

The algorithm for the kinetic Monte Carlo simulation of CO oxidation reaction over Pd(1 1 0) is similar [34,35] to that applied for Pt(1 0 0), Scheme 1. In the case of Pd(1 1 0) each lattice cell (the size of the lattice N was varied from 500 to 8000) can exist in one of five intermediate states: *, CO_{ads}, O_{ads}, [$^*O_{sub}$], [CO_{ads}/O_{sub}]). After each choice of one of the processes and an attempt to realize it, the program considered the internal diffusion cycle that involved M diffusion attempts for CO_{ads} molecules (usually $M = 50$–100). The reaction rate of CO oxidation and the surface coverages (θ_O, θ_{CO}, θ_{Osub}) were calculated after each MC step as a ratio of the amount of CO_2 molecules formed (or the number of lattice cells in the corresponding state) to the overall amount of cells N^2 [34,35]. A drastic increase in the reaction rate occurs simultaneously with the removal of the CO_{ads} layer and filling the surface with the O_{ads} layer. When the rate approaches its maximal value, the concentration of adsorbed oxygen redistributes: $O_{ads} \rightarrow O_{sub}$. The position of the maximum on the curve of the subsurface oxygen concentration determines the moment of a decrease in the reaction rate. Simultaneously, the surface accumulates CO_{ads} and this process is accompanied by the complete O_{ads} removal. The lowest reaction rate level is associated with the $CO_{ads} + O_{sub}$ interaction. A decrease in the concentration (O_{sub}) to a certain critical value again creates favorable conditions for the reaction, and this completes the oscillation cycle. Changes in the coverages occur *via* the propagation of the mobile "oxygen waves", whose front is characterized by the high concentration of catalytically active sites responsible for the maximal rate of CO_2 molecule formation.

Table 1
The values of the rate coefficients (s^{-1}) for the elementary steps of the Scheme 2.

k_1	k_2	k_{-2}	k_4	k_5	k_6	k_{-6}	k_7
1	1	0.2	0.03	0.01	1	0.5	0.02

The following values of the rate coefficients (s^{-1}) given in Table 1 have been chosen for simulations.

It is known that CO and O_2 adsorption leads to the added/missing row reconstruction of the Pd(1 1 0) plane $(1 \times 1) \rightarrow (1 \times 2)$ (Fig. 7A and B). As a result, the diffusion of CO_{ads} molecules along the rows of metals atoms occurs faster than across the rows. Fig. 8A represents dissipative structures of dynamic spiral waves in the reaction of CO oxidation on Pd(1 1 0) obtained by PEEM [33]. Fig. 9 shows the modeled waves evolution after changes the isotropic regime ($M_x/M_y = 50/50$) to the anisotropic one ($M_x/M_y = 80/20$). Observed asymmetric behaviour of the spiral waves agrees with experimental data displayed in Fig. 8A. It is clearly seen that the spiral wave observed in the experiment reflects the anisotropy of the Pd(1 1 0) surface in the direction [1 $\bar{1}$ 0]. The detailed modeling of such structures was described in [35].

3.3. Modeling of target patterns on Pd(1 1 0) with surface defects

We obtained the simulation results concerning the influence of surface defects on a spatio-temporal dynamics during the oscillation regime. The single defect (d) was considered as a spot of the 10×10 active centres in size, having kinetic properties distinct from the clean Pd(1 1 0) surface. It was proposed that the kinetic parameters are: $k_1(d) = 3k_1(s^{-1})$ and $k_{-2}(d) = 3k_{-2}(s^{-1})$. Isotropic diffusion intensity $M = 20$ is taken for both the surface and defect. So-called "target" patterns (concentric waves arising from a small region of the surface called "pacemaker" [9]) have been observed experimentally in numerous studies, e.g., [36]; we tried to reproduce such a patterns in simulation. Remarkably, the nucleation of a concentric wave took place exclusively at the surface defect thus suggesting that the "pacemaker" region exhibits a high catalytic activity. The 1st concentric wave immediately displays an isotropy and at larger propagation distances start up a 2nd and 3rd concentric waves (Fig. 10). The frequency of wave front generation can be changed by changing the control parameters. Hence, the defects of the real surfaces, characterized by distinctive adsorption and kinetic properties, indeed influences on the spatio-temporal organization of the adsorbed layer during the oscillations, and serves as a source of specific structures on the surface ("target"-type in our case).

3.4. Palladium nanoparticles: modeling of CO spillover and wave patterns

The mechanism of local oscillator synchronisation is one of the significant problems of the oscillatory behaviour of catalytic reactions [19]. The isothermal kinetic oscillations in different oxidation reactions are observed as a rule [19,37] on the supported metals and on metal tips considered as a superposition of the interrelated nanoplane surfaces. It was found that on the single crystal surfaces and supported metal catalysts the following factors should play the dominant role in synchronizing a catalytic system consisting of isolated oscillators with distinctive properties: (i) the global coupling

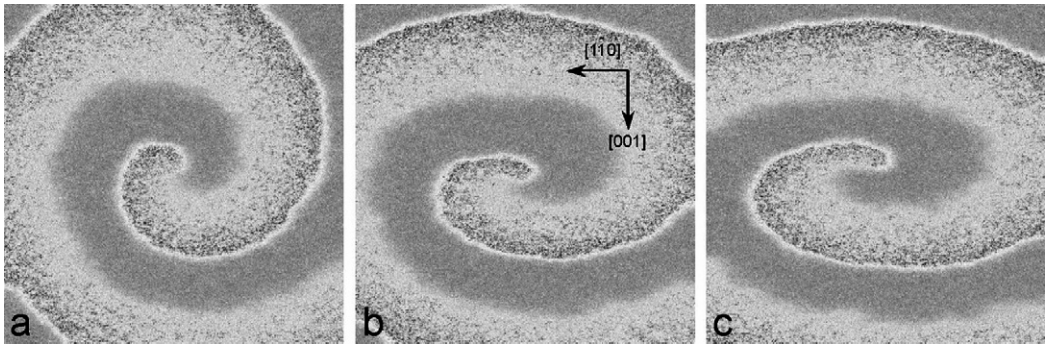

Fig. 9. Changes in the form of the spiral wave in the CO oxidation reaction on the Pd(1 1 0) surface after the transition from the regime with isotropic diffusion (M_x/M_y = 50/50) to anisotropic (M_x/M_y = 80/20), N = 1536: (a) isotropic diffusion; (b) after the first turn of the spiral; (c) after the second turn of the spiral.

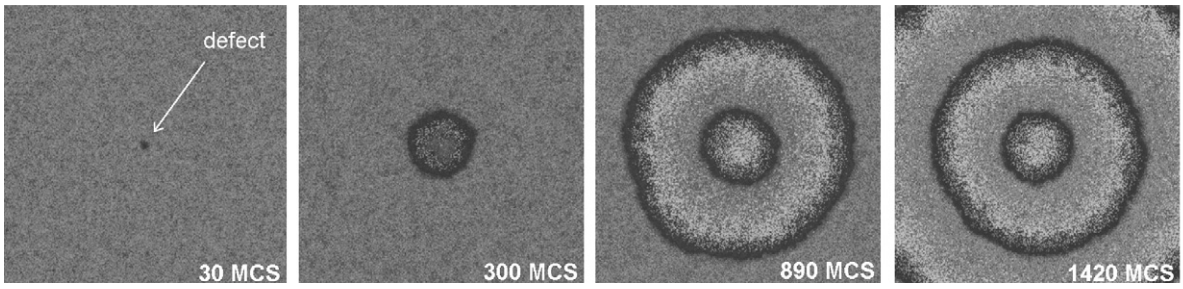

Fig. 10. Evolution of the target waves starting from the central spot (10 × 10 active centers in size). The size of the lattice is 1000 × 1000. Adsorbed oxygen is painted black, subsurface oxygen – bright, adsorbed carbon monoxide – gray.

through the gas phase; (ii) the coupling *via* heat transfer [38, and ref. therein]. In the case of the nanoparticle-, tip-surfaces the diffusion of the adsorbed species can be responsible primarily for the synchronisation of local oscillators. Furthermore, according to Boudart [10] considering the kinetic features of CO oxidation reaction over Pd/Al_2O_3 it is necessary to take into account the contribution of CO_{ads} diffusion over the support onto the active metal nanoparticles ("reverse"-spillover).

An attempt has been made to model the oscillatory behaviour of the $CO + O_2$ reaction over the supported Pd nanoparticle. Thereto we combine the usual kinetic Monte Carlo approach to model the reaction and the stochastic model for the imitating the supported nanoparticle with dynamically changing surface morphology [39,40]. It is evident that the reaction kinetics on a supported metal catalyst might be quite different as compared to that on the single crystal surfaces, as a result of interplay between different planes present on nanoparticles [9,19,41]. Here we take into account the "reverse"-spillover phenomena [42]. CO can adsorb both over the Pd surface and the support (desorption coefficient of CO_{ads} from the support was assumed four times higher than that from the Pd particle) and then diffuse through the support to the Pd particle giving the additional source of CO_{ads} flux to the particle through its perimeter. Oxygen can adsorb only on the available centers of the Pd particle (Boudart model [10]), preferably on the terrace sites.

Fig. 11 shows the results of simulation for different sizes of the supported nanoparticles. It is seen that decreasing of the particle linear size from 200 × 200 to 20 × 20 lead to the disappearing of oscillations. The reasons for this phenomenon are the following: (i) decreasing of the particles size attended by the roughening (reduction well-defined faceting and increasing of step-edge/defect sites concentration) of its surface and, hence, to the deficit of the active centres for oxygen adsorption; (ii) the influence of the additional flux of CO_{ads} from the perimeter that shifts the interval of oscillations to the higher value of $P_{(O_2)}$. The presence of CO_{ads} spillover determines the character of concentration waves over the surface of Pd nanoparticle: (i) oxygen wave propagates from the central region of the particle to the perimeter, (ii) CO_{ads} wave moves in opposite direction—from the perimeter, always enriched by CO_{ads} concentration, to the centre of the particle. Fig. 12 illustrates this process. The simulated frames correspond to the case shown on Fig. 11 with initial particle size 50 × 50 × 10 atoms. The particle was preliminary roughened at T = 500 K [39,40]. At MCS = 4860 the surface of the particle is covered by CO_{ads} and O_{sub}–the low reaction rate. The free active sites available for the oxygen adsorption appear on the Pd surface due to slow reaction between CO_{ads} and O_{sub}, MCS = 4910. The oxygen wave propagates over the Pd surface, MCS = 4940, the high reaction rate. Then CO_{ads} wave moves from the perimeter, always enriched by CO_{ads} supplying from the support, to the centre

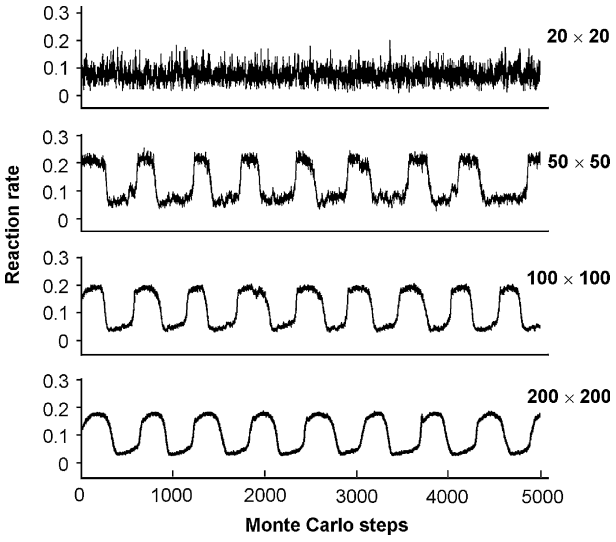

Fig. 11. Reaction rate dependencies vs. Monte Carlo steps (time) for different sizes of the supported particle.

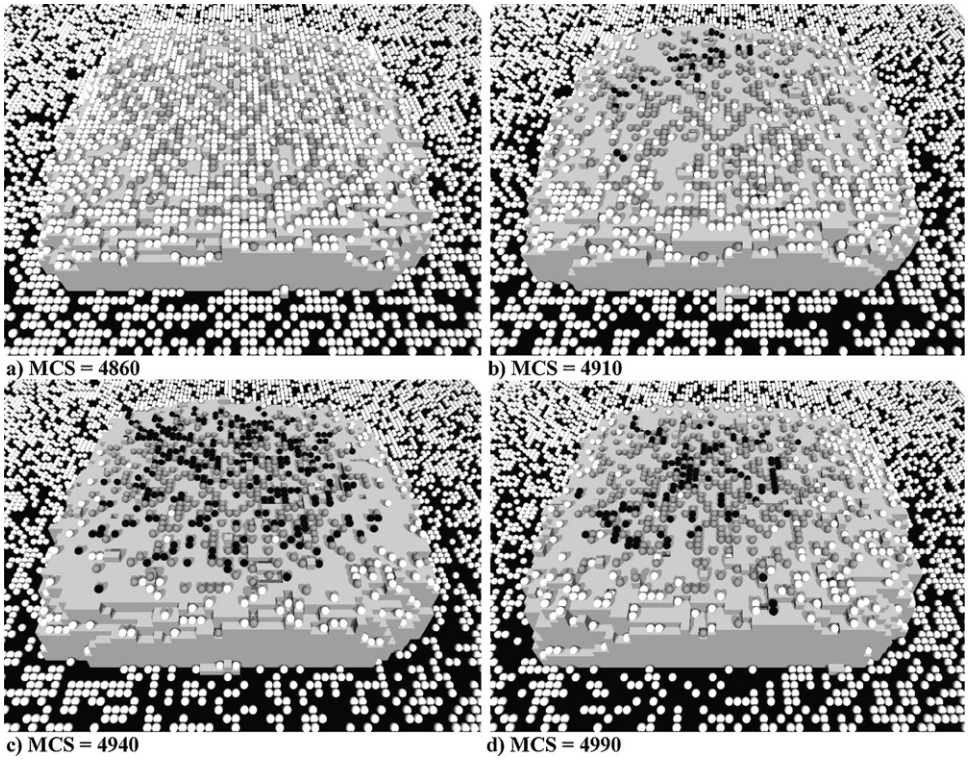

Fig. 12. Dynamics of the adsorbed layer on the supported Pd particle in the course of oscillations. Support surface is painted black, the particle – gray, CO_{ads} adsorbed both on the particle and on the support – white balls, O_{ads} atoms – black balls, O_{sub} – dark grey balls.

of the particle, MCS = 4990, the $CO_{ads} + O_{sub}$ layer forms again and the cycle is completed.

4. Conclusion

The $CO + O_2$ reaction on the Pt and Pd surfaces is surprisingly complex. We have explored different metal surfaces (single crystals, tips, nanoparticles) and have observed varied reaction regimes: steady-state, oscillatory, waves, spillover. Special attention was payed to spectral (HREELS) and mass-spectrometric (TPR, TDS) data, revealing the details of interaction of molecular, atomic and subsurface states of oxygen with carbon monoxide that is very important for the creation of physicochemical models for the satisfactory explanation of self-oscillations and surface waves in heterogeneously catalyzed reactions. The experimental results show the comparison of molecular and atomic adsorbed oxygen on Pt(1 0 0)–(hex) and Pt(1 0 0)–(1×1) and its activity in the interaction with CO_{ads} in low temperature region. The absence of interaction of O_{2ads} with CO_{ads} is evident, therefore we do not include in the detailed mechanism the steps concerned with the formation of the so-called "hot" oxygen atoms. CO_2 formation on the Pt surface is a result of the interaction between CO_{ads} molecules and O_{ads} atoms. The FEM studies on the Pt-tip surface demonstrate that the self-oscillations and waves propagation are connected with periodic changes in the surface structure of nanoplane (1 0 0)–(hex) $\leftrightarrow (1 \times 1)$, varying catalytic property of metal. The low temperature adsorption and reaction between carbon monoxide and oxygen on the Pt(1 0 0)–(hex) and Pt(1 0 0)–(1×1) surfaces were investigated using HREELS and TPR to learn the details of the reaction dynamics at these catalytic surfaces. The Pt(1 0 0)–(1×1) surface are catalytically active for the CO oxidation due to their ability to dissociate O_2 molecules. TPR results from $CO_{ads} + O_{ads}$ coadsorption experiments on (1×1) directly support the conclusion that CO_{ads} react with oxygen atoms at low temperature (140–200 K) to form CO_2. The Pt(1 0 0)-*nano*plane reconstruction was reported for the first time for the Pt-tip surface by means of Field Ion Microscopy (FIM) investigation with a resolution of ~2 Å. The Pt(1 0 0)–(1×1) *nano*surface ($\sim 10^4$ atoms) was prepared by low temperature field evaporation of the Pt(1 0 0)-oriented tip at 78 K. The FIM observation on Pt tip shows that the clean (1 0 0)–(1×1)-surface was metastable and transformed thermally activated back into the (*hex*)-phase above 270 K [43]. For comparison, the clean Pt(1 0 0)–(1×1) single crystal surface was found to reconstruct into (hex) at $T \sim 370$ K [44]. The observed sharp decreasing of the phase transformation temperature Pt(1 0 0)–(hex) $\rightarrow (1 \times 1)$ in the case of *nano*plane surface ($\sim 10^4$ atoms) compared with the single crystal surface ($\sim 10^{15}$ atoms) is one of the typical examples of the "*structure gap*" manifestation. It could be expected the possibility of the self-oscillatory CO oxidation regimes on the Pt(1 0 0) *nano*plane surface at $T \sim 300$ K, and it was experimentally observed in our studies by FEM.

In contrast to the Pt(1 0 0) surface, the clean Pd(1 1 0) surface does not change its surface structure during catalytic CO oxidation. PEEM, TPR and MB studies demonstrate the formation of the subsurface oxygen O_{sub}, which is an important intermediate species in the $CO + O_2$ oscillatory reaction on a Pd(1 1 0). The original isothermal TD-spectra shows that the reactivity of $^{18}O_{sub}$ situated in the subsurface layer of Pd(1×2) is noticeably lower than that of atomic layer $^{16}O_{ads}$. These results confirm the proposed reaction mechanism (subsurface oxygen route, Scheme 2) served as a base for the kinetic Monte Carlo simulations of oscillations and surface waves including the spiral waves. The agreement between experimental and theoretical results gives rise to the formulation of new model with the point defect ("pacemaker"). In the course of simulations the formation of the so-called "target" patterns having the shape of the concentric waves formed periodically on the "pacemaker", which has been observed experimentally by PEEM.

FEM microscopy has been used as an *in situ* catalytic flow reactor in the 10^{-7} to 10^{-3} mbar total pressure to investigate the dynamics (self-oscillation, waves) of the surface phenomena associated with CO oxidation on a nanoscale level. The experimental results on Pt- and Pd-tip surfaces demonstrate that the maximum rate of CO_2 formation is attained in a travelling narrow zone between O_{ads} and CO_{ads} layers. In this reaction zone the highest concentration of free active centres is reached, which contribute to dissociative adsorption of O_2 and a rapid reaction with closely arranged CO_{ads} and O_{ads} species. Our FEM results indicated a key role of reaction-diffusion waves includes the participation of the different crystal nanoplanes and indicates an effective coupling of adjacent planes. It becomes possible to study catalysis on a nanoscale level, which is necessary for the understanding of the mechanism of action of the highly dispersed supported metal catalysts having metal nanocrystallites 100–300 Å in size as active parts of the catalyst. The reaction of CO with oxygen on nanoplanes of the tip surface is an example of the direct microscopic observation of mass transfer process ("spillover") during catalytic reaction.

As far as we know, there is no published experimental data on the observation of the isothermal chemical waves in the CO oxidation reaction on the Pd nanoparticles. Stimulus for the simulation of the CO oxidation dynamics on the nanoparticle surface serves the experimental observation of the possibility of local self-oscillations and "fast waves" on the nanoplane of Pt(1 0 0), $\sim 100 \times 100$ atoms in size, situated on the tip surface surrounded by CO_{ads} layer, adsorbed on the neighboring nanoplanes of different crystallographic structure. Size-dependent catalytic properties of the supported nanoparticles has been studied by Monte Carlo in an effort to shed light on cluster size and support effects at non-linear kinetics: CO oxidation on the Pd/support model catalysts is a "reverse" spillover sensitive.

The statistical lattice models have been constructed that described the oscillation and wave dynamics in the adsorbed layer for the reaction of CO oxidation over the Pt(1 0 0) and Pd(1 1 0) single crystal surfaces. These models differ in the mechanisms of formation of oscillations: a mechanism involving the phase transition of planes (Pt(1 0 0): (hex) $\leftrightarrow (1 \times 1)$) and a mechanism with the formation of subsurface oxygen, (Pd(1 1 0)). The models demonstrate the oscillations of the rate of CO_2 formation, the surface coverage and the appearance of surface waves. The great interest in self-oscillatory phenomena in oxidation reactions over metal surfaces is for a large part caused by the possibility to perform the catalytic processes more efficiently using unsteady-state operation. The comprehensive study of CO, O_2 adsorption and $CO + O_2$ reaction in a row: single crystals $\rightarrow$ tips $\rightarrow$ nanoparticles have shown the same nature of active centers over these metal surfaces. The presence of CO_{ads} "reverse"-spillover determines the character of concentration waves over the surface of Pd nanoparticle: (i) oxygen wave propagates from the central region of the particle to the perimeter; (ii) CO wave moves in the opposite direction.

The dissociation of oxygen is the first step in CO oxidation and determines the measured reactivity, which is the number of produced CO_2 molecules per active center ($\sim 10^{15}$ centers for PEEM, $\sim 10^4$ centers for FEM). It is evident that the similar character of the wave rising and propagation on the single crystal (PEEM) and on the tips (FEM) is governed both by the similar nature of the active centers and their reactivity (similar adsorption rates of reagents (CO, O_2) and the rates of CO_2 formation). The fundamental result of this work is that the non-linear reaction kinetics is not restricted to macroscopic planes since: (i) the planes $\sim$200 Å in diameter shows the same non-linear kinetics; (ii) the regular waves appears under the reaction rate oscillations; (iii) the propagation of reaction-diffusion waves includes the participation of the different crystal nanoplanes and indicates an effective coupling of adjacent planes.

Acknowledgements

This work was supported by the RFBR Grants # 08-03-00454 and 08-03-00825.

References

[1] G. Ertl, Dynamics of reactions at surfaces, Adv. Catal. 45 (2000) 1–69.
[2] R. Imbihl, G. Ertl, Oscillatory kinetics in heterogeneous catalysis, Chem. Rev. 95 (1995) 697–733.
[3] M.M. Slin'ko, N.I. Jaeger, Oscillating heterogeneous catalytic systems, in: B. Delmon, J.T. Yates (Eds.), Studies in Surface Science and Catalysis, 86, Elsevier, Amsterdam, 1994, p. 393.
[4] J.L. Gland, M.R. McClellan, F.R. McFeely, Carbon monoxide oxidation on the kinked Pt(3 2 1) surface, J. Chem. Phys. 79 (1983) 6349–6356.
[5] A. Borg, A.M. Hilmen, E. Bergene, STM studies of clean, CO- and O_2-exposed Pt(1 0 0)–hex–RO.7°, Surf. Sci. 306 (1994) 10–20.
[6] T. Matsushima, The mechanism of the CO_2 formation on Pt(1 1 1) and polycrystalline surfaces at low temperatures, Surf. Sci. 127 (1983) 403–423.
[7] A. Hopkinson, X.-C. Guo, J.M. Bradley, D.A. King, A molecular beam study of the CO induced surface phase transition on Pt(1 0 0), J. Chem. Phys. 99 (1993) 8262–8269.
[8] P.D. Cobden, N.M.H. Janssen, Y. van Breugel, B.E. Nieuwenhuys, Non-linear behaviour in the NO–H_2 reaction over single crystals and field emitters of some Pt-group metals, Faraday Discuss. 105 (1996) 57–72.
[9] V.V. Gorodetskii, V.I. Elokhin, J.W. Bakker, B.E. Nieuwenhuys, Field electron and field ion microscopy studies of chemical wave propagation in oscillatory reactions on platinum group metals, Catal. Today 105 (2005) 183–205.
[10] M. Boudart, Model catalysts: reductionism for understanding, Topics Catal. 13 (2000) 147–149.
[11] V.I. Elokhin, E.I. Latkin, A.V. Matveev, V.V. Gorodetskii, Application of statistical lattice models to the analysis of oscillatory and autowave processes in the reaction of carbon monoxide oxidation over platinum and palladium surfaces, Kinet. Catal. 44 (2003) 692–700.
[12] M.Yu. Smirnov, D. Zemlyanov, V.V. Gorodetskii, E.I. Vovk, Formation of the mixed $(NO + CO)/(1 \times 1)$ islands on the Pt(1 0 0)–(hex) surface, Surf. Sci. 114 (1998) 409–422.
[13] V. Gorodetskii, J.H. Block, W. Drachsel, M. Ehsasi, Oscillations in the carbon monoxide oxidation on platinum surfaces observed by field electron microscopy, Appl. Surf. Sci. 67 (1993) 198–205.
[14] P.D. Cobden, V.V. Gorodetskii, B.E. Nieuwenhuys, Field emission microscope study of the initial behaviour of the palladium–hydrogen system at low temperatures, Surf. Sci. 432 (1999) 61–68.
[15] Yu. Suchorski, R. Imbihl, V.K. Medvedev, Compatibility of field emitter studies of oscillating surface reactions with single crystal measurements: catalytic CO oxidation on Pt, Surf. Sci. 401 (1998) 392–399.
[16] V.V. Gorodetskii, W. Drachsel, Kinetic oscillations and surface waves in catalytic $CO + O_2$ reaction on Pt surface: field electron microscope, field ion microscope and high resolution electron energy loss spectroscope studies, Appl. Catal. A: Gen. 188 (1999) 267–275.
[17] P.R. Norton, J.A. Davies, D.K. Creber, C.W. Sitter, T.E. Jackman, The Pt(1 0 0)$(5 \times 20) \leftrightarrow (1 \times 1)$ phase transition: a study by Rutherfold backscattering, nuclear microanalysis, LEED and thermal desorption spectroscopy, Surf. Sci. 108 (1981) 205–234.
[18] H.H. Rotermund, Self-organized reactions on surfaces, Phys. Scr. T49 (1993) 549–553.
[19] V. Gorodetskii, J. Lauterbach, H.-H. Rotermund, J.H. Block, G. Ertl, Coupling between adjacent crystal planes in heterogeneous catalysis by propagating reaction diffusion waves, Nature 370 (1994) 276–279.
[20] E. Ritter, R.J. Behm, G. Potschke, J. Wintterlin, Direct observation of a nucleation and growth process on an atomic scale, Surf. Sci. 181 (1987) 403–411.
[21] R.J. Behm, P.A. Thiel, P.R. Norton, G. Ertl, The interaction of CO and Pt(1 0 0). I. Mechanism of adsorption and Pt phase transition, J. Chem. Phys. 78 (1983) 7437–7447.
[22] J. Schmidt, Ch. Stuhlmann, H. Ibach, Oxygen adsorption on the Pt(1 1 0)–(1×2) surfaces studied with EELS, Surf. Sci. 284 (1993) 121–128.
[23] H.P. Bonzel, G. Broden, G. Pirug, Structure sensitivity of NO adsorption on a smooth and stepped Pt(1 0 0) surface, J. Catal. 53 (1978) 96–105.
[24] R. Martin, P. Gardner, A.M. Bradshaw, The adsorbate-induced removal of the Pt{1 1 0} surface reconstruction. Part II: CO, Surf. Sci. 342 (1995) 69–84.
[25] Y.-S. Lim, M. Berdau, M. Naschitzki, M. Ehsasi, J.H. Block, Oscillating catalytic CO oxidation on a platinum field emitter tip: determination of a reactive phase diagram by field electron microscopy, J. Catal. 149 (1994) 292–299.
[26] M. Eiswirth, R. Schwankner, G. Ertl, Conditions for the occurrence of kinetic oscillations in the catalytic oxidation of CO on a Pt(1 0 0) surfaces, Z. Phys. Chem. 144 (1985) 59–67.
[27] R. Imbihl, M.P. Cox, G. Ertl, H. Müller, W. Brenig, Kinetic oscillation in the catalytic CO oxidation on Pt(1 0 0): theory, J. Chem. Phys. 83 (1985) 1578–1587.
[28] R. Imbihl, M.P. Cox, G. Ertl, Kinetic oscillations in the catalytic CO oxidation on Pt(1 0 0): experiments, J. Chem. Phys. 84 (1986) 3519–3534.
[29] E.I. Latkin, V.I. Elokhin, V.V. Gorodetskii, Monte Carlo model of oscillatory CO oxidation having regard to the catalytic properties due to the adsorbate-induced Pt(1 0 0) structural transformation, J. Mol. Catal. A: Chem. 166 (2001) 23–30.

[30] V.V. Gorodetskii, A.V. Matveev, A.V. Kalinkin, B.E. Nieuwenhuys, Mechanism for CO oxidation and oscillatory reactions on Pd tip and Pd(1 1 0) surfaces, Chem. Sustain. Dev. 11 (2003) 67–74.
[31] J.-W. He, P.R. Norton, Thermal desorption of oxygen from a Pd(1 1 0) surface, Surf. Sci. 204 (1988) 26–34.
[32] V.V. Gorodetskii, A.V. Matveev, E.A. Podgornov, F. Zaera, Study of the low-temperature reaction between CO and O_2 over Pd and Pt surfaces, Topics Catal. 32 (2005) 17–28.
[33] J.H. Block, M. Ehsasi, V. Gorodetskii, A. Karpowicz, M. Berdau, Direct observation of surface mobility with microscopic techniques: photoemission electron and field electron microscopy, in: T. Inui, et al. (Eds.), New Aspects of Spillover Effect in Catalysis: Studies in Surface Science and Catalysis, vol. 77, Elsevier Science Publ. B.V, 1993, pp. 189–194.
[34] E.I. Latkin, V.I. Elokhin, A.V. Matveev, V.V. Gorodetskii, The role of sub-surface oxygen in oscillatory behaviour of $CO+O_2$ reaction over Pd metal catalysts: Monte Carlo model, J. Mol. Catal. A: Chem. 158 (2000) 161–166.
[35] E.I. Latkin, V.I. Elokhin, V.V. Gorodetskii, Spiral concentration waves in the Monte Carlo model of CO oxidation over Pd(1 1 0) caused by synchronization via CO_{ads} diffusion between separate parts of catalytic surface, Chem. Eng. J. 91 (2003) 123–131.
[36] J. Wolff, M. Stich, C. Beta, H.H. Rotermund, Laser-induced target patters in the oscillatory CO oxidation on Pt(1 1 0), J. Phys. Chem. B 108 (2004) 14291–14292.
[37] J. Lauterbach, G. Bonilla, T.D. Pletcher, Non-linear phenomena during CO oxidation in the mbar pressure range: a comparison between Pt/SiO_2 and Pt(1 0 0), Chem. Eng. Sci. 54 (1999) 4501–4512.
[38] M.M. Slinko, A.A. Ukharskii, N.I. Jaeger, Global and non-local coupling in oscillating heterogeneous catalytic reactions: the oxidation of CO on zeolite supported palladium, Phys. Chem. Chem. Phys. 3 (2001) 1015–1021.
[39] E.V. Kovalyov, E.D. Resnyanskii, V.I. Elokhin, B.S. Bal'zhinimaev, A.V. Myshlyavtsev, Novel statistical lattice model for the supported nanoparticle. Features of the reaction performance influenced by the dynamically changed shape and surface morphology of the supported active particle, Phys. Chem. Chem. Phys. 5 (2003) 784–790.
[40] E.V. Kovalyov, V.I. Elokhin, A.V. Myshlyavtsev, Stochastic simulation of physicochemical processes performance over supported metal nanoparticles, J. Comput. Chem. 29 (2008) 79–86.
[41] V.P. Zhdanov, Impact of surface science on the understanding of kinetics of heterogeneous catalytic reactions, Surf. Sci. 500 (2002) 966–985.
[42] M.A. Röttgen, S. Abbet, K. Judai, J.-M. Antonietti, A.S. Wörz, M. Arenz, C.R. Henry, U. Heiz, Cluster chemistry: size-dependent reactivity induced by reverse spill-over, J. Am. Chem. Soc. 129 (2007) 9635–9639.
[43] T.T. Tsong, Atom-probe Field Ion Microscopy, Cambridge University Press, Cambridge, 1990.
[44] K. Kuhnke, K. Kern, G. Comsa, Preparation and thermal stability of the clean metastable Pt(1 0 0)–(1×1) surface: a thermal energy helium scattering study, Surf. Sci. 343 (1995) 44–52.